



## LAND SUBSIDENCE MODELLING RESEARCH

Receiving Institution: AGH University of Science and Technology,  
Cracow, Poland.  
Faculty of Mining Surveying and Environmental Engineering

Supervisor: Dr. Eng. Agnieszka Malinowska,  
Associate Professor

Trainee: Ahmed Wedam Ahmed  
Sending Institution: Ataturk University, Turkey  
Erasmus, 2019.

# **Land subsidence modelling caused by groundwater withdrawal in Bogdanka Coal Mines, Poland.**

## **ABSTRACT**

Land subsidence is a threat that occurs worldwide as a result of the withdrawal of fluids and also underground mining. The subsidence is mainly due to excessive groundwater withdrawal from certain types of rocks, such as fine-grained sediments. Mitigating the effects of land subsidence generally requires careful observations of the temporal change of groundwater level and ideally modelling of groundwater flow and subsidence. The aim of groundwater modelling for Bogdanka Coal Mine is to forecast the values of ground subsidence induced by water withdrawal due to progressing mining operations that will occur on the terrain surface. In the work reported here, a novel numerical solution based on consolidation theory was developed in MATLAB to predict the land subsidence of the Bogdanka Coal Mine. In order to adjust the model to the local conditions historical data from the study area for the first year 1976 and subsidence measurements between 1982-2010 were used. The presented solution allowed for subsidence model development which can support the prediction of the ground movement for the Bogdanka Coal Mines to forecast the values of subsidence in the Jura aquifer for the period up to 2042.

## 1. Introduction

Land subsidence occurs when groundwater has been withdrawn from certain types of rocks such as fine-grained sediments. The rock compacts due to the pressure decrease in the aquifer strata (Perlman 2018). Eliminating the adverse effects of land subsidence requires observations on the temporal change of elevation coupled with groundwater flow modelling (Özyurt *et al.* 2018). In the areas where excessive groundwater is withdrawal and from susceptible aquifer systems, land subsidence induced by aquifer-system compaction is typically observed, resulting in severe socio-economic damage for the affected communities. Generally, it is the lowered groundwater levels caused by groundwater pumping that causes land subsidence in compressible aquifer systems. Such systems typically make up of basin-fill and unconsolidated alluvial layers that include both aquifers and aquitards (Galloway and Burbey 2011). Either slow or sudden, the motion of the ground due to subsidence is a hazard that threatens civil and environmental resources. Present and potential future hazards have been assessed by models that are based on basic relations between groundwater levels or aquifer hydraulic head, effective or intergranular stress, the compressibility of groundwater and the aquifer skeleton, and groundwater flow (Özyurt *et al.* 2018). These models use two different approaches: the first is based on groundwater flow theory (Jacob 1950, 1940) and secondly, the theory of linear poroelasticity (Biot 1941). Various models implementing i.e. the “De Glee” method and software programs like the IMOD have been used to simulate land subsidence (Guzy *et al.* 2018). Globally, land subsidence is a consequence of the over-exploitation of groundwater resources from susceptible aquifer systems. According to an assessment, measured subsidence rates in different locations in the world range from 6 mm/year in Kolkata, India between 1992-1998 and 300 mm/year in Mexico City, Mexico between 2004-2006 (Osmanoğlu *et al.* 2011). And among 18 selected sites distributed globally the mean and median subsidence rate is 100 mm/year and 55 mm/year respectively (Özyurt *et al.* 2018).

This research reported here seeks to use MATLAB software to model and predict the land subsidence of the KCB. MATLAB predictive analytics uses historical data to predict future events. Typically, historical data is used to build a mathematical model that captures important trends. That predictive model is then used on current data to predict what will happen next or to suggest actions to take for optimal outcomes. Predictive analytics has received a lot of attention in recent

years due to advances in supporting technology, particularly in the areas of big data and machine learning (Anon. 2019).

## 2. Study Area

Bogdanka Coal Mine is located in eastern Poland, 30 km northeast from Lublin (Figure 1). The total, current mine area has 77.39 Km<sup>2</sup>. The terrain surface is mainly rural area, occupied by cultivated fields, meadows, pastures and forest. The landscape of the research area varies poorly, with small denizens reaching up to 10 m. Elevation ranges from 165m to 168m a.m.s.l. (Guzy, 2017)

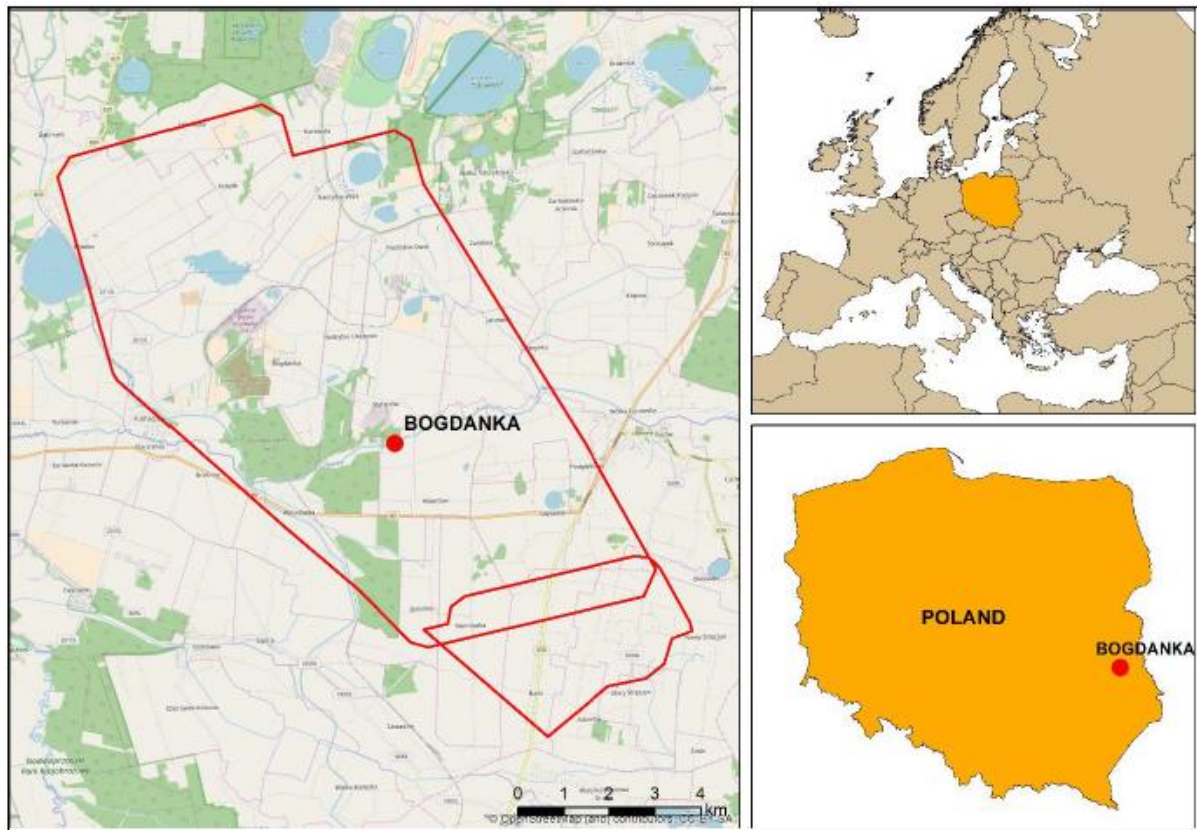


**Figure 2.1 Bogdanka Coal Mine – research area location (Source; Guzy 2017, Modelling of ground subsidence due to water withdrawal)**

## 2.1. Geological and hydrogeological conditions

In the research area, one can distinguish 5 geological layers differing in geological and hydrogeological conditions (Figure 2). The layers are as follows (from uppermost to lowermost):

- Quaternary – with the thickness between 0-100 m, build mainly from soft soils, that is to say sands, silts, loams and gravels;
- Chalk – with the thickness up to 300 m, build from impermeable limestone, marlstone and dolomite;
- Albin – with the thickness between 0-10 m, build mainly from fractured sandstone;
- Jura – with the thickness up to 100m, build mainly from limestone and sandstone;
- Carbon – with the thickness between 20-400 m or more (unrecognized depth), build from carbon, sandstone and siltstone.

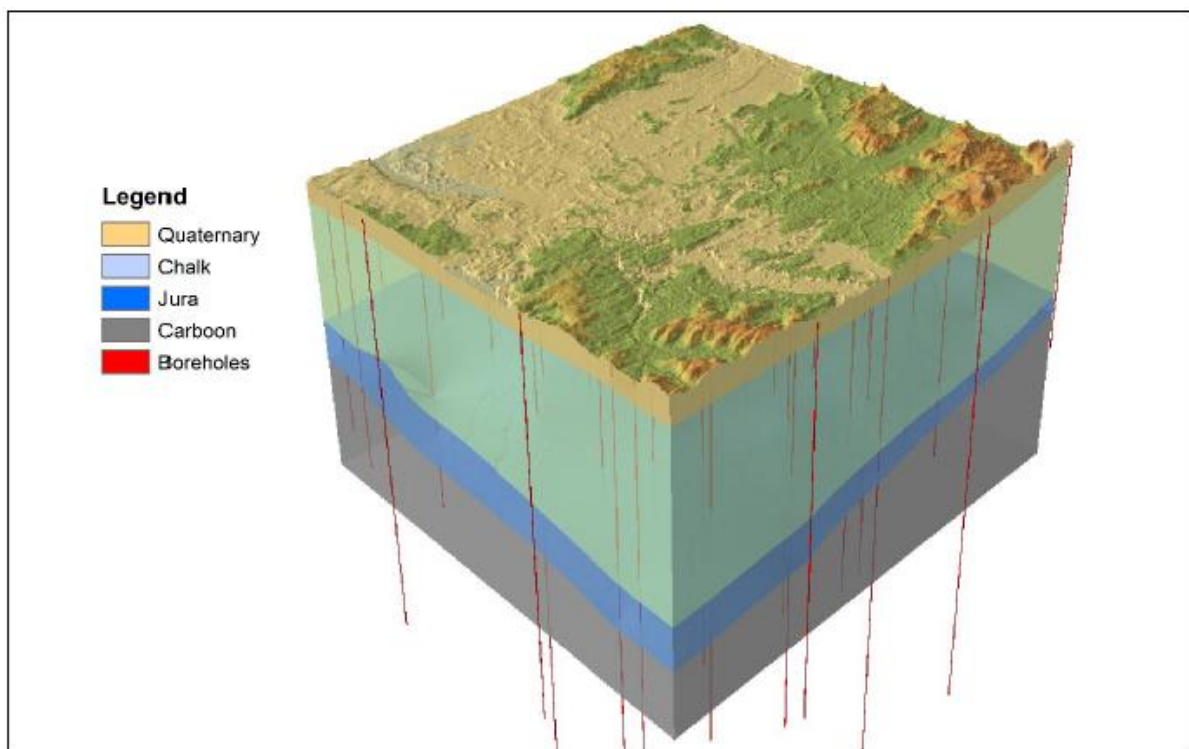


**Figure 2.2. Geological conditions in Bogdanka Coal Mine – 3D perspective (Source; Guzy, 2017, Modelling of ground subsidence due to water withdrawal)**

The main aquifer in the research area is considered to be the lower part of Jura and the uppermost strata of Carbon, overall of the thickness up to 100 m. This aquifer consists mainly of sandstone and has a

behaviour of fractured hard rock mass. The second aquifer is Albin layer with similar geological conditions to Jura aquifer.

The geological connections between Jura aquifer and the terrain surfaces are not recognised, although, due to high thickness of impervious limestone and marlstone strata in Chalk layer, one can say there is no water inflow from Quaternary into deep, geological strata including Jura aquifer. (Guzy, 2017)

## 2.2. Coal exploitation

Coal exploitation started in 1982 and currently is carried out at the depth of 785 m u.m.s.l. Coal is extracted in mining panels that have the length up to 1000 m and the width up to 250 m, thickness of exploited seam varies between 1,4-2,0 m. From 1982 to 2017 coal has been exploited in mining panels located in northern and partly central part of mine area. Up to 2042 it is planned to carry out the mining operations in southern part of the research area (Figure 3). (Guzy, 2017)

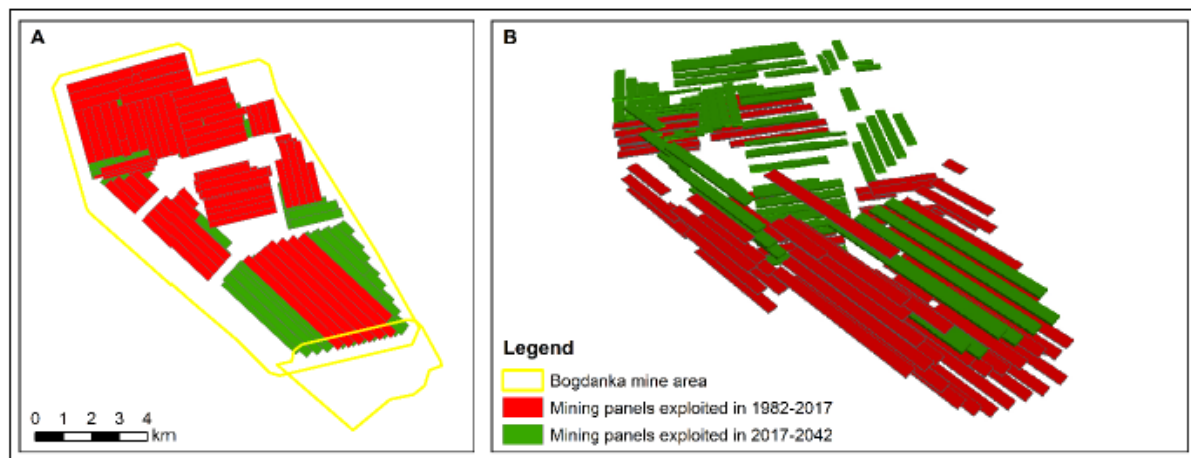


**Figure 2.3. Coal exploitation in Bogdanka Coal Mine – A: 2D perspective, B: 3D perspective (Source; Guzy, 2017, Modelling of ground subsidence due to water withdrawal)**

## 2.3. Water extraction

Water extraction in the research area had started in 1976, 4 years before first mining operations exploiting coal started. Water is extracted mainly from the bottom of Jura aquifer (via 2 mining shafts) and from Carbon, where flows from underlying, upper lying and lateral geological strata via fractures into mining panels and further, by mining corridors reaches 4 mining shafts from which is extracted to the terrain surface (Figure 4). To monitor changes in water level in Jura

during coal exploitation, 44 piezometers had been placed in this aquifer before water pumping started in 1976. Observed in 2010 values of depression cone in Jura reached maximum 533 m in the drainage centrum (Figure 4).

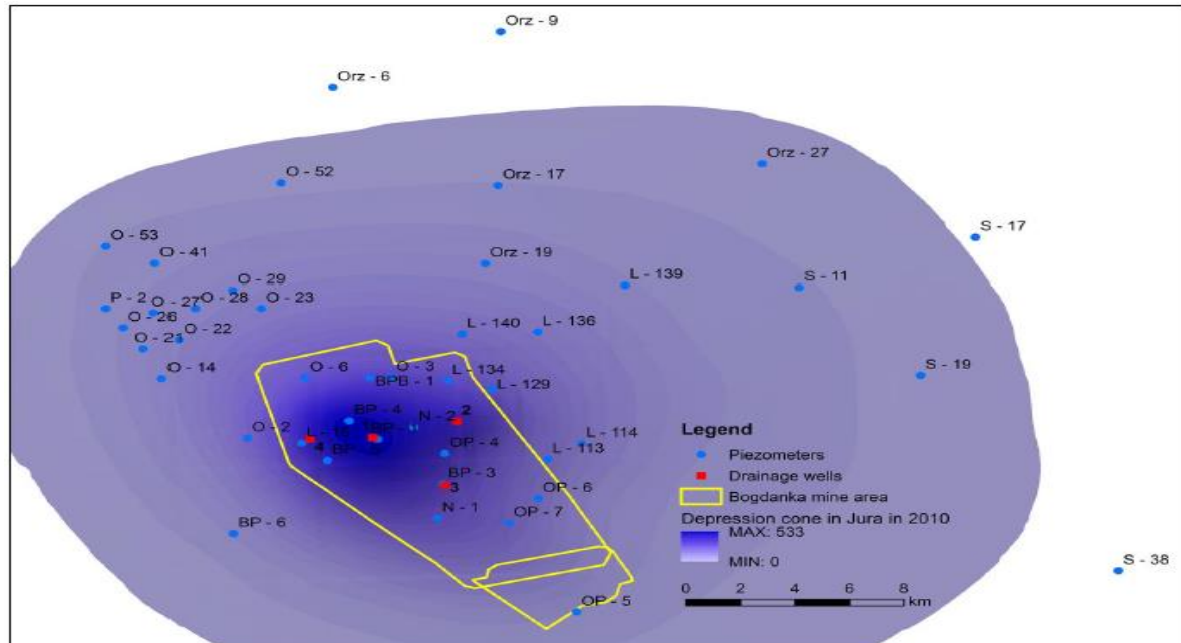


Figure 2.4. Extraction wells and piezometric localisation in the research area in the background of depression cone in Jura in 2010 (Source; Guzy, 2017.)

Table 2.1. Mechanical rock mass strata properties in the research area

Stratigraphy	Lithology	Rock mass strata properties							
		Compression strength in drained state [Mpa]	Compression strength in hydrated state [Mpa]	Tensile strength [MPa]	Young's modulus [MPa]	Poisson's ratio	Water content [%]	Volume density [g/cm <sup>3</sup> ]	Porosity [%]
Chalk	marlstone	6,75	3,09	0,56	1233	0,05	19,43	1,70	38,90
	chalk	29,44	15,14	1,54	4712	0,06	7,88	2,14	21,51
	limestone	32,32	19,46	2,16	5207	0,05	6,56	2,22	19,20
	sandstone	5,60	0,60	0,60	-	-	5,98	2,28	15,30
Jura	limestone	21,05	16,14	2,30	4304	0,08	7,56	2,20	20,30
	sandstone	17,57	13,57	1,61	3930	0,09	9,62	2,16	23,40
	limestone	37,26	26,76	2,53	7164	0,06	8,82	2,22	19,40
	claystone	7,59	6,09	0,74	2087	0,13	10,22	2,11	23,10

(Source; Guzy, 2017.” Modeling of ground subsidence due to water withdrawal”)



### 3. Methodology



**Fig. 3.1 Methodology Chart**

**\*New altered model based on Cc calculations using in situ porosity for final results.**

#### **Breakdown**

The research and analysis began with the continuation of the estimation for land subsidence with the aid of Terzaghi's 1 D theory of soil consolidation. The idea in improving the research was to Use MATLAB to be able to iterate results or aid in predicting future occurrence of the land subsidence (extent to which the vertical consolidation will occur).



Data obtained for the Bogdanka field assuming for the year 1976 was used. The Jura aquifer had various porosity recordings at different layers available amongst the data provided.

From Terzaghi's equation, Subsidence,  $S = \frac{\Delta e}{e_i + 1} * D$  (1)

Where  $\Delta e$ = Change in void ratio,  $e_i$ = initial void ratio and D is the aquifer thickness;

Therefore, we had to convert porosity n, to the void ratio e. this was done using the Equation 2;

$$e = \frac{n}{n-1} \quad (2)$$

The initial porosities available for the various layers in the Jura aquifer were used in calculating the various initial void ratios.

$$\text{Change in void ratio} = \text{Initial void ratio } (e_i) - \text{Final void ratio } (e_f) \quad (3)$$

### 3.1. Change in Porosity converted to change in void ratio

Final porosity and Initial porosity was determined and their difference as the change in porosity calculated and converted to Change in void ratio using Equation 2.

Final Porosity( $n_f$ ) was estimated to be in the range between 0.85 to 0.90 of the initial porosity ( $n_i$ ). Calculations were made with the interval of 0.01 from .85 to .90 of the initial porosity for the various layers in Jura. The mean for each layer calculated for as the  $n_f$  of each layer.

Having known the  $n_i$ , the Change in porosity was calculated for, as Change in Porosity= Initial Porosity,  $n_i$  – Final Porosity,  $n_f$ .

### 3.2. Subsidence Calculation

Having estimated  $e_i$ , change in void ratio and using a thickness D of 10m; subsidence at various layers in Jura were calculated for using Equation 1.

### 3.3. Subsidence as a function of Time

After calculating the subsidence for the period, this then aided in predicting the future occurrence by developing a model for the known period under review. This was done using Eq. (4) with reference from Koppejan (1948):

$$S = \left( \left( \frac{1}{C_p} + \frac{1}{C_s} * \log t \right) \ln \left( \frac{P_i + \Delta p_i}{P_i} \right) * \right) D \quad (4)$$

However, the consolidation constants  $C_p$  and  $C_s$ , initial pressure ( $p_i$ ) and change in pore pressure ( $\Delta p_i$ ) will be required to make the calculations. Since values for change in void ratio and initial void ratios were clearly available in the data acquired for the study area a relationship with initial void ratio  $e_i$  and change void ratio  $\Delta e$  was used, replacing the initial pressure and the change in pore pressure resulting to Eq. (5):

$$S = \left( \left( \frac{1}{C_p} + \frac{1}{C_s} * \log t \right) * \left( \frac{\Delta e * C_c}{(e_i + 1)^2} \right) * \right) D \quad (5)$$

$C_c$  calculated using equation 6 and 7;

$$C_c = 0.29(e_i - 0.27) \quad (6)$$

$$C_c = 0.43(e_i - 0.25) \quad (7)$$

Min and Max subsidence estimated were used in Establishing two fundamental simultaneous equations in evaluating  $C_s$ .

Having developed the various variable in Equation 5 and assuming  $C_p=1$ , possible min and max subsidence for an extensive period spanning from 1976 to 2010 was predicted.

However, predicted subsidence values compared with previous data had inconsistencies.

Upon further research equation for the  $C_c$  considering initial porosity given was used in establishing a new value for the variable  $C_s$ .

$$C_c = \frac{N_o}{371.747 - 4.275N_o} \quad (8)$$

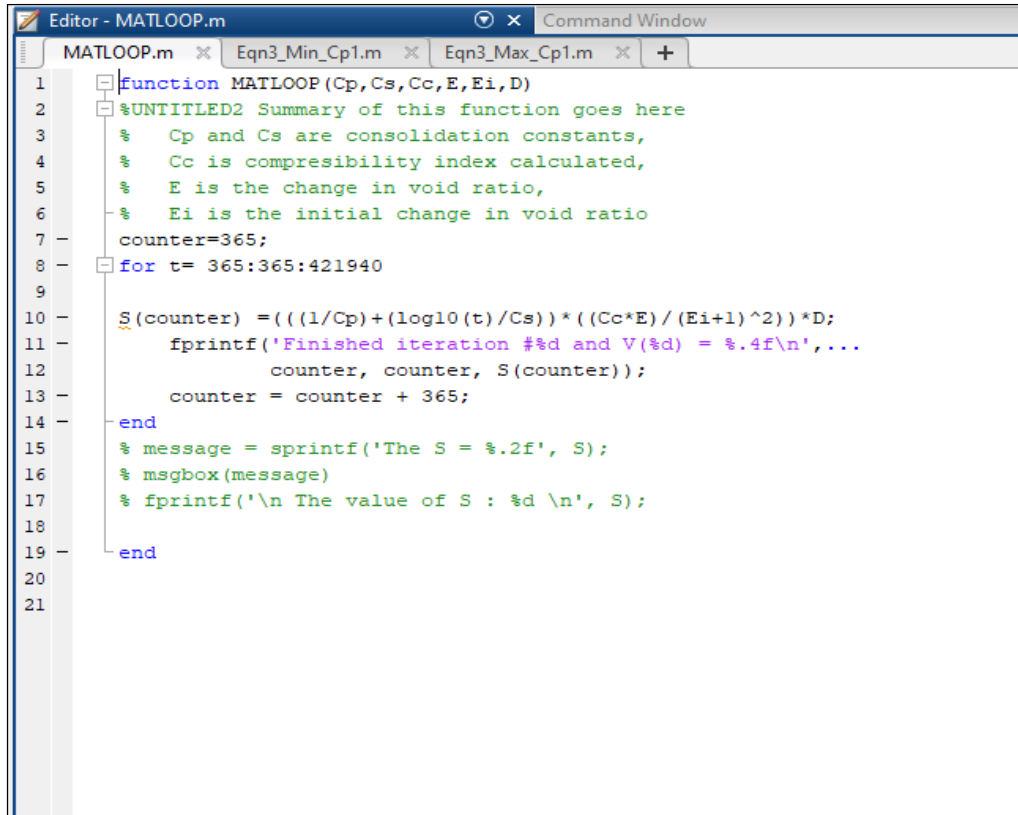
Where  $n_o$  is initial porosity (in situ porosity)

Considering the min and max subsidence; the initial porosity at these layers where used in determining the  $C_c$  and consequently establishing the simultaneous equation as previously done and the new  $C_s$ , calculated for.

## 4. Results and Discussions

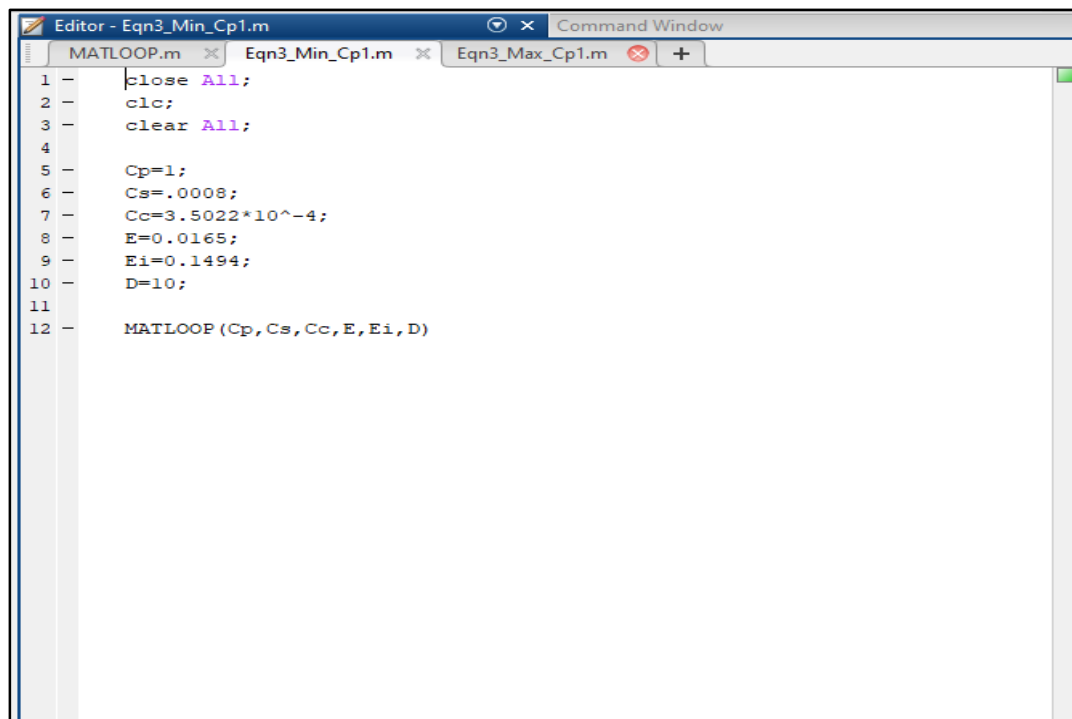
### 4.1. Results

#### 4.1.1 MATHLAB Coding



```
Editor - MATLOOP.m
MATLOOP.m  Eqn3_Min_Cp1.m  Eqn3_Max_Cp1.m  +
1  function MATLOOP(Cp,Cs,Cc,E,Ei,D)
2  %UNTITLED2 Summary of this function goes here
3  % Cp and Cs are consolidation constants,
4  % Cc is compresibility index calculated,
5  % E is the change in void ratio,
6  % Ei is the initial change in void ratio
7  counter=365;
8  for t= 365:365:421940
9
10     S(counter) = (((1/Cp)+(log10(t)/Cs))*((Cc*E)/(Ei+1)^2))*D;
11     fprintf('Finished iteration #%d and V(%d) = %.4f\n',...
12             counter, counter, S(counter));
13     counter = counter + 365;
14 end
15 % message = sprintf('The S = %.2f', S);
16 % msgbox(message)
17 % fprintf('\n The value of S : %d \n', S);
18
19 end
20
21
```

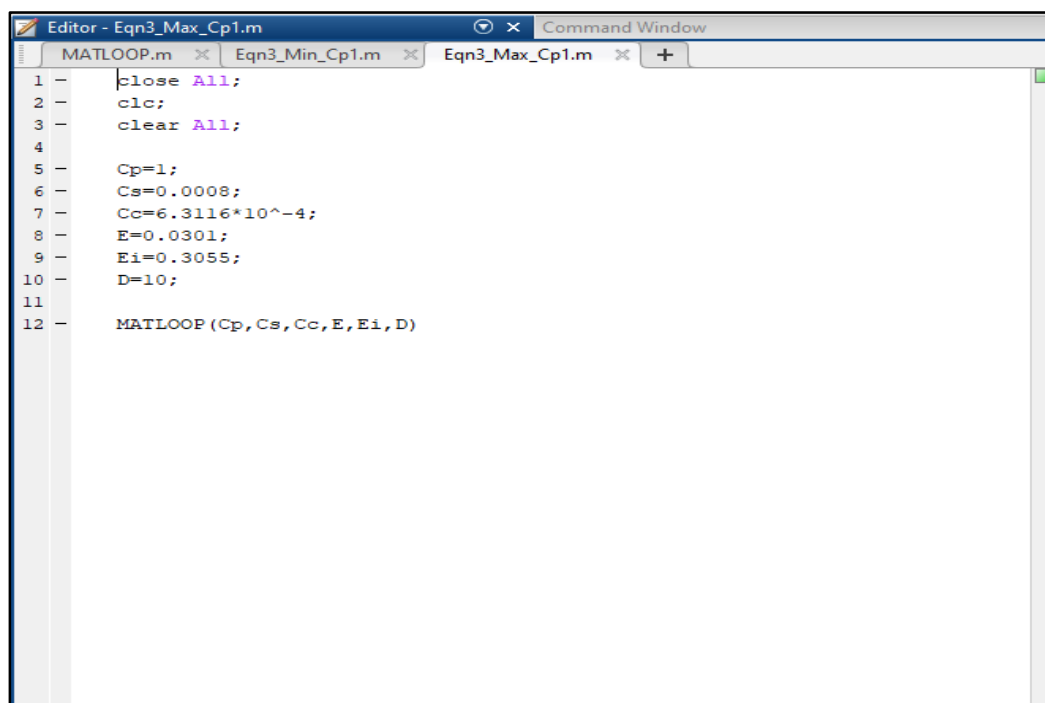
Figure 4.1. Loop generated for Subsidence as a function of time calculation



The image shows a MATLAB Editor window with the title bar 'Editor - Eqn3\_Min\_Cp1.m'. The Command Window is also visible. The code in the editor is as follows:

```
1 - close All;  
2 - clc;  
3 - clear All;  
4  
5 - Cp=1;  
6 - Cs=.0008;  
7 - Cc=3.5022*10^-4;  
8 - E=0.0165;  
9 - Ei=0.1494;  
10 - D=10;  
11  
12 - MATLOOP (Cp,Cs,Cc,E,Ei,D)
```

**Figure 4.2. Minimum Subsidence Calculation**



The image shows a MATLAB Editor window with the title bar 'Editor - Eqn3\_Max\_Cp1.m'. The Command Window is also visible. The code in the editor is as follows:

```
1 - close All;  
2 - clc;  
3 - clear All;  
4  
5 - Cp=1;  
6 - Cs=0.0008;  
7 - Cc=6.3116*10^-4;  
8 - E=0.0301;  
9 - Ei=0.3055;  
10 - D=10;  
11  
12 - MATLOOP (Cp,Cs,Cc,E,Ei,D)
```

**Figure 4.3. Maximum Subsidence Calculation**

#### 4.1.2. Model Generated;

For Min Sub prediction;

$$S = 0.0238 \ln(x) + 0.1401 \quad (9)$$

$R^2 = 1$ ; logarithmic regression

For Max Sub prediction;

$$S = 0.0605 \ln(x) + 0.3571 \quad (10)$$

$R^2 = 1$ ; logarithmic regression

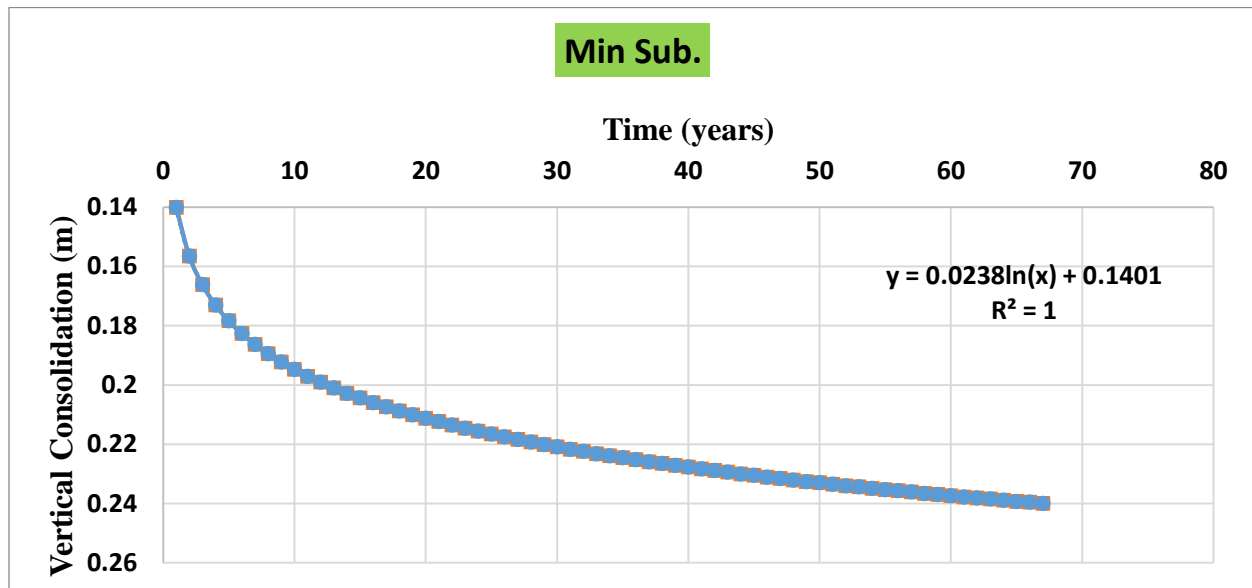


Figure 4.4. Graph of min sub prediction

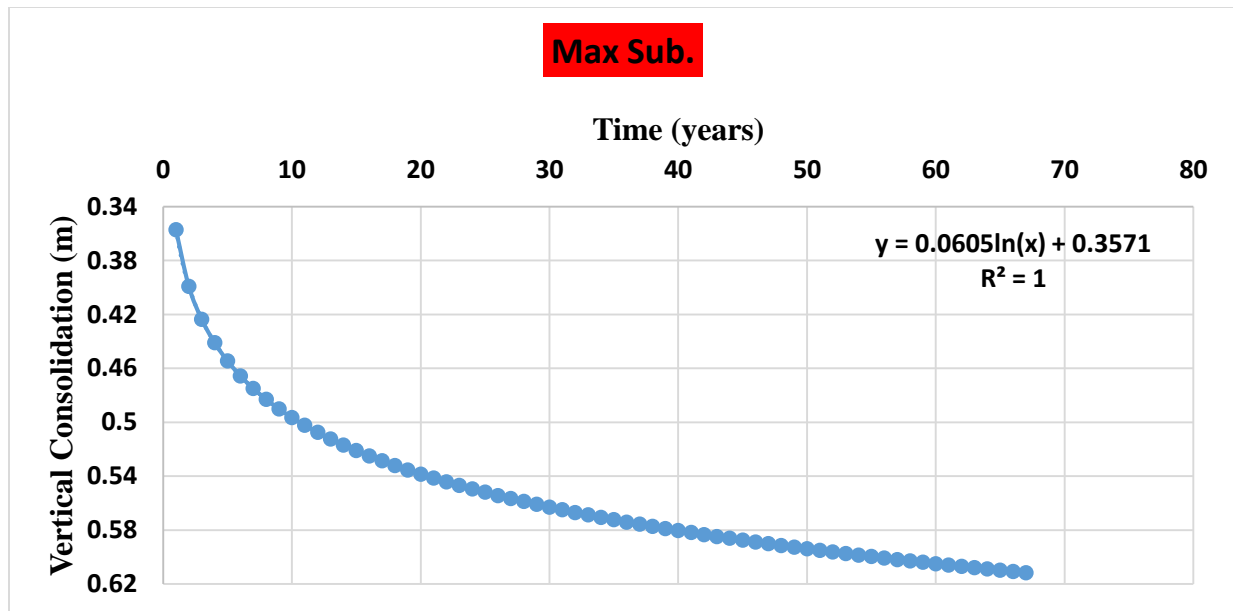


Figure 4.5. Graph for max sub prediction

#### 4.1.3. Estimated Predictions (m)

Table 4.1

<u>Year</u>	<u>1976</u>	<u>1982</u>	<u>1984</u>	<u>1986</u>	<u>2010</u>	<u>2024</u>	<u>2042</u>
Min	0.1401	0.1863	0.1923	0.1971	0.2246	0.2326	0.24
Max	0.3571	0.4749	0.4901	0.5022	0.5723	0.5926	0.6116

#### 4.1.4. Measured Subsidence (m)

Table 4.2

<u>Year</u>	<u>1982</u>	<u>1984</u>	<u>1986</u>	<u>2010</u>
Min	0.01699	0.01623	0.01457	0
Max	0.101411	0.18158	0.20212	0.57235

(from QGIS Data, Artur 2017)

## 4.2. Discussion

The subsidence results obtained (estimated) were compared with related land subsidence from previous research using subsidence results measured within the year 1982 – 2010 as shown in Table 4.2.

Cs value ( $7.8011 \times 10^{-4}$ ) used for predicting the Min subsidence resulted in approximately consistent values with reference data whereas the Cs value used for predicting that of Max subsidence produced unfavorable (incomparable) results.

However, in altering the Cs value for max sub equation from the initial value of  $12.3807 \times 10^{-4}$  to  $11 \times 10^{-4}$  and finally to  $8 \times 10^{-4}$ ; predicted values resulted in more reasonable and comparatively similar subsidence value with literature (i.e., observed max sub in 2010 to be 0.572m in both measurement).

The minimum and maximum subsidence to be observed were plotted and a general line regression analysis was done to obtain a strong  $R^2$  value. Linear regression, exponential regression, logarithmic regression, polynomial regression, and power regression were used. Logarithmic regressions resulted in  $R^2$  values of 1 in both cases of Cc for minimum and maximum subsidence whereas the other regression analysis had  $R^2$  values less than 1. Therefore, in calculating the minimum level of subsidence the model generated for a logarithmic regression was Eq.9 as shown in Fig. 4.4.

In calculating the maximum level of subsidence, the model generated for a logarithmic regression was Eq. 10 as shown in Fig. 4.5.

## 5. Conclusions

The research focused on Terzaghi soil consolidation theory and subsidence as a function of time with MATLAB in the iteration analysis. With the subsidence, compressibility index and consolidation constants predicted, for the study area, the values for minimum subsidence using the year 1976 as starting point with regards to the forecasting as a reference point; minimum subsidence is predicted to be approximately 0.14m whereas the maximum land subsidence is predicted to be 0.47m assuming the groundwater withdrawal is the same as the rate of water



recharge into the aquifer. Consequently, in 2010, the predicted maximum subsidence of approximately 0.57m is estimated just as in the measured subsidence values in Table 4.2 and therein, as the main goal was for the futuristic prediction of subsidence, the similarity in the prediction for 2010 estimated a prediction of minimum subsidence and maximum subsidence of approximately 0.23m and 0.59m respectively for the year 2024. Moreover, for the year 2042, an estimated prediction of 0.24m and 0.61m of minimum subsidence and maximum subsidence respectively. However, it is highly recommended that further accurate data concerning porosity, moisture content, compressibility index and effective stress of the field be obtained for more accurate subsidence results for a three dimensional consideration.

Finally, yet importantly, consolidation constants should also be measured and identified from the laboratory. Results can then be used to predict the trend of land subsidence with a given lifespan of the study area.

## References

- Anon., 2019, Predictive Analytics. <https://www.mathworks.com/discovery/predictive-analytics.html>. Accessed: 25 March, 2019.
- Biot, M. A., 1941, General theory of three-dimensional consolidation. *Journal of Applied Physics*, 12(2), 155–164. doi:10.1063/1.1712886.
- Caló, F., Notti, D., Galve, J., Abdikan, S., Görüm, T., Pepe, A., and Balik Şanlı, F., 2017, Dinsar-based detection of land subsidence and correlation with groundwater depletion in konya plain, turkey. *Remote Sensing*, 9(1), 83.
- Canaslan Comut, F., Lazecky, M., Ustun, A., and Yalvack, S., 2015, Land Subsidence Detection in Agricultural Areas of Konya Closed Basin by PS-InSAR and GNSS Observations. *FRINGE 2015*, 731, 5.
- De Glopper, R. J., and Ritzema, H. P., 2006, Land subsidence. *Drainage Principles and Applications*, 16, 477-512.
- Galloway, D., and Burbey, T. J., 2011, Review: Regional land subsidence accompanying groundwater extraction. *Hydrogeology Journal*, 19(8), 1459–1486. doi:10.1007/s10040-011-0775-5.
- Guzy, A., Ahmed, A. W., and Malinowska, A., 2018, Spatio-Temporal Distribution of Land Subsidence and Water Drop Caused by Underground Exploitation of Mineral Resources. *International Multidisciplinary Scientific GeoConference: SGEM: Surveying Geology & mining Ecology Management*, 18, 467-476.

Habibbeygi, F., Nikraz, H., and Verheyde, F., 2017, Determination of the compression index of reconstituted clays using intrinsic concept and normalized void ratio. *International Journal of GEOMATE*, 13(39), 54-60.

Hoffman, J., Leake, S. A., Galloway, D. L., and Wilson, A. M., 2003, MODFLOW-2000 ground-water model—User guide to the subsidence and aquifer-system compaction (SUB) package: U.S. Geological Survey Open-File Report 2003-233, 44 p., <http://pubs.usgs.gov/of/2003/ofr03-233/>, Accessed: 15 Oct, 2019.

Jacob, C. E., 1950, Flow of ground water. In: Rouse H (ed), *Engineering hydraulics*. Proceedings of the Fourth Hydraulics Conference, Iowa Institute of Hydraulic Research, Iowa City, IW.

Jacob, C. E., 1940, On the flow of water in an elastic artesian aquifer. *American Geophysical Union*.

Osmanoğlu, B., Dixon, T. H., Wdowinski, S., Cabral-Cano, E., and Jiang, Y., 2011, Mexico City subsidence observed with persistent scatterer InSAR. *International Journal of Applied Earth Observation*, 13(1), 1–12. doi:10.1016/j.jag.2010.05.009.

Özyurt, N. N., Avcı, P., and Bayarı, C. S., 2018, Using Groundwater Flow Modelling for Investigation of Land Subsidence in the Konya Closed Basin (Turkey). *Handbook of Research on Trends and Digital Advances in Engineering Geology*, 569-590.

Perlman, H. A., 2018, Land subsidence, USGS Water Science School. <https://water.usgs.gov/edu/earthgwlandsubside.html>. Accessed: 18 June 2018.

Terzaghi, K., Peck, R. B., and Mesri, G., 1967, *Soil Mechanics in Engineering Practice*, John Wiley & Sons. Inc., New York.

Üstün, A., Özkan, İ., Bildirici, İ. Ö., Tuşat, E., Üstüntaş, T., Eren, Y., and Özdemir, A., 2014, Monitoring and Investigating the Causes of Land Subsidence in Konya Closed Basin with Geodetic Methods. TÜBİTAK Project No: 110Y121 (Turkish).

Üstün, A., Özkan, İ., Tuşat, E., Eren, Y., Bildirici, İ. Ö., Üstüntaş, T., and Özdemir, A., 2013, Monitoring and Investigating the Causes of Land Subsidence in Konya Closed Basin with Geodetic Methods. TÜBİTAK Research Project, Interim report, Konya, 110 (Turkish).

Üstün, A., Tuşat, E., Yalvaç, S., Özkan, İ., Eren, Y., Özdemir, A., Bildirici, İ. Ö., Üstüntaş, T., Kırtıloğlu, O. S., and Mesutoğlu, M., 2015, Land subsidence in Konya Closed Basin and its spatio-temporal detection by GPS and DInSAR. *Environmental Earth Sciences*, 73(10), 6691-6703.

Yavuz, S., 2010, Determination of Karst Properties in the Konya-Karapınar Basin Using Hydrogeological Parameters, Master Thesis, Cukurova University, Graduate School of Natural and Applied Sciences, Adana (Turkish).